Design of D-R system for improving transmission efficiency of Cassegrain antenna

WENXIN CHENG[1], SHENGHAO LI[1], MIAOFANG ZHOU[2], PING JIANG[1], HUAJUN YANG[1,*]
[1]*School of Physics, University of Electronic Science and Technology of China, Sichuan Province 610054, China*
[2]*School of Physics and Electronic Science, Changsha University of Science and Technology, Changsha Province 410114, China*

The occlusion of the secondary mirror will reduce the transmission efficiency of the traditional Cassegrain antenna. In this paper, a double reflection (D-R) system is designed to improve the transmission efficiency of Cassegrain antenna. Based on the three-dimensional vector reflection theorem, the influence of parameters and practical factors on transmission efficiency are analyzed in detail. According to our simulation results, the optimized D-R system can improve the transmission efficiency of traditional Cassegrain antenna up to 97.42% after taking some practical factors such as dispersion, chamfering, radius of incident beam, spindle deviation, reflectivity and transmittance into consideration. In addition, the transmission efficiency of the whole system is higher than the transmission efficiency of the traditional Cassegrain antenna under an axis offset between 0 and 20.34 mm. Compared with other complex antenna systems, our proposed system possesses a relatively simple structure, and is more practical in improving the transmission efficiency of traditional Cassegrain antenna.

(Received June 8, 2023; accepted February 12, 2024)

Keywords: Cassegrain antenna, Three-dimensional vector refraction and reflection theorem, Space optical communication

1. Introduction

Cassegrain antenna is one of the most common antennas in optical communication. Improving the transmission efficiency of Cassegrain antenna can promote the development of optical communication. After research, it is discovered that the reflection shielding in the optical center leads to the loss of energy in this part, which greatly reduces the efficiency of optical communication [1-4]. Therefore, it has been studied by many predecessors and different schemes have been proposed, but there are some drawbacks. The solution of minimizing the shielding effect of by calculating the minimum shielding diameter of the Cassegrain antenna reflector [5] cannot essentially solve the problem. The scheme of distributing the incident beam around the aperture through multiple reflections of a single telephoto re-entrant cutting prism [6,7] is complex in principle and difficult to operate in practice. Consequently, it has been proposed that the solid beam can be converted into a hollow beam, such as Laguerre Gaussian (LG) beams [8] and a conic lens pair [9], but too many optical components lead to loss of transmission efficiency due to factors such as wavelength.

In this paper, a D-R system is designed to improve the transmission efficiency of traditional Cassegrain antenna. The three-dimensional vector reflection theorem and MATLAB are utilized for analyzing. The main steps of this paper are as follows: firstly, the principle and disadvantage of traditional Cassegrain antenna is introduced; secondly, the schematic structure of the D-R system is proposed and the parameters of D-R system are analyzed; thirdly, the influence of several practical factors such as dispersion, chamfering, radius of incident beam, spindle deviation, reflectivity and transmittance on the transmission efficiency of the whole system are analyzed in detail; finally, the transmission efficiency of the whole system is obtained.

2. Analysis of traditional Cassegrain antenna

Through a series of devices [10], the incident beam is converted into a ring-collimated beam that enters the Cassegrain antenna consisting of two reflective surfaces of the primary and secondary mirrors. As shown in Fig. 1, the incident beam is converted into a hollow beam by passing through the Cassegrain antenna, but the central part of the light is reflected back after reaching the secondary mirror, resulting in energy loss. Since the energy of this collimated beam obeys Gaussian distribution, the traditional Cassegrain antenna loses a large amount of energy.

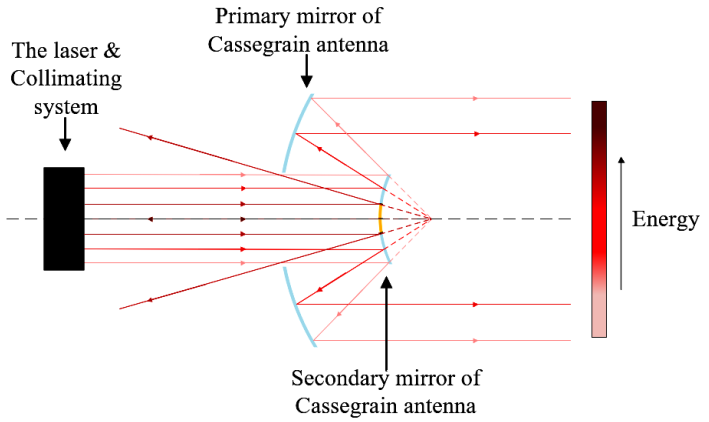

Fig. 1. Defects in the transmission process of traditional Cassegrain antenna (color online)

3. Design and analysis of D-R system

To avoid the huge energy loss in the center of the antenna, a D-R system is designed in front of the antenna to convert the solid beam into a hollow beam. The transmitting antenna with D-R system is shown in Fig. 2.

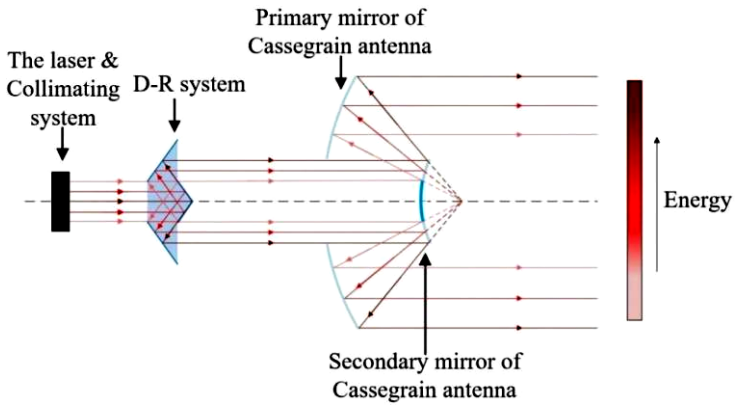

Fig. 2. Schematic diagram of transmitting antenna system with D-R system (color online)

As can be seen in Fig. 2, the beam transforms from solid to hollow after the D-R system, and passes completely through the Cassegrain antenna. Due to the rotational symmetry of the device, the two-dimensional diagram can be used for further analysis. The D-R system after a reasonable parameter setting is shown in Fig. 3.

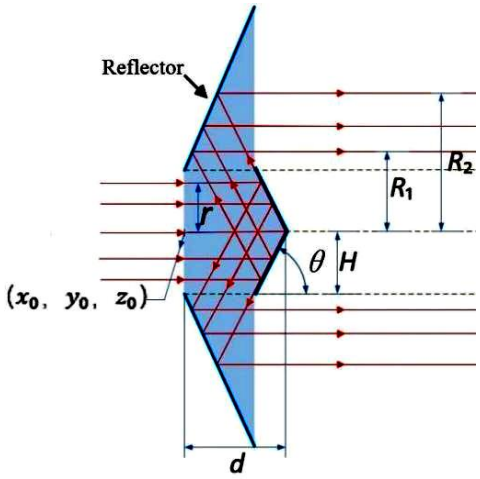

Fig. 3. Structural diagram and parameter design of the D-R system (color online)

As shown in Fig. 3, the whole part of the D-R system consists of a common lens material with the incident and exit planes perpendicular to the optical axis, ensuring that the light beam enters and exits the device perpendicularly.

The two reflective surfaces are parallel to each other, and the fiber optic mirrors encapsulated on them make the incident light achieve total reflection and finally reach the exit plane of the optical axis in parallel. The surface equation of the D-R system is shown in Eq. (1).

$$\begin{cases} \dfrac{(y-y_0)^2}{d^2}+\dfrac{(z-z_0)^2}{d^2}=3(1-\dfrac{x-x_0}{d})^2 \\ \dfrac{(y-y_0)^2}{H^2}+\dfrac{(z-z_0)^2}{H^2}=(\sqrt{3}\dfrac{x-x_0}{H}+1)^2 \end{cases} \tag{1}$$

The three-dimensional simulation of the structure of the D-R system can be simulated by the two-dimensional diagram of the D-R system and the surface equations, as shown in Fig. 4.

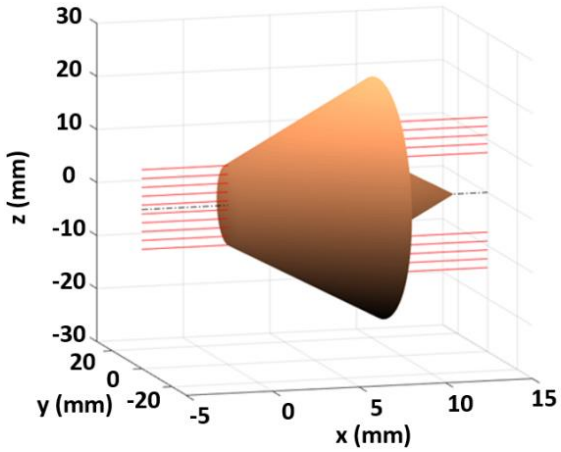

Fig. 4. Three-dimensional simulation of beam passing through D-R system (color online)

In order to meet the requirements of the lens in the Cassegrain antenna, the radius of the exit beam should be less than 15 mm and the hollow radius should be greater than 2.996 mm [11,12]. On the basis of the three-dimensional vector reflection theorem, the relationship between the parameters expressed in Eqs. (2) and (3).

$$R_1=H+(d-\frac{r}{\tan\theta}+\frac{H+r}{\tan 2\theta})\frac{\tan\theta\tan 2\theta}{\tan 2\theta-\tan\theta} \tag{2}$$

$$R_2=R_1+r \tag{3}$$

According to the above relationships, the radius of the incident beam r is set as 7.5 mm. To ensure that the device can accessas as much of the beam as possible, the value of H is set as 7.5 mm. The values of the parameters θ and d are somewhat limited due to the beam passing through the two reflectors. The simulation diagrams of the relationship between R_1, R_2, θ, d are shown in Fig. 5, which provides a more visual representation of the effect of the parameters on each other.

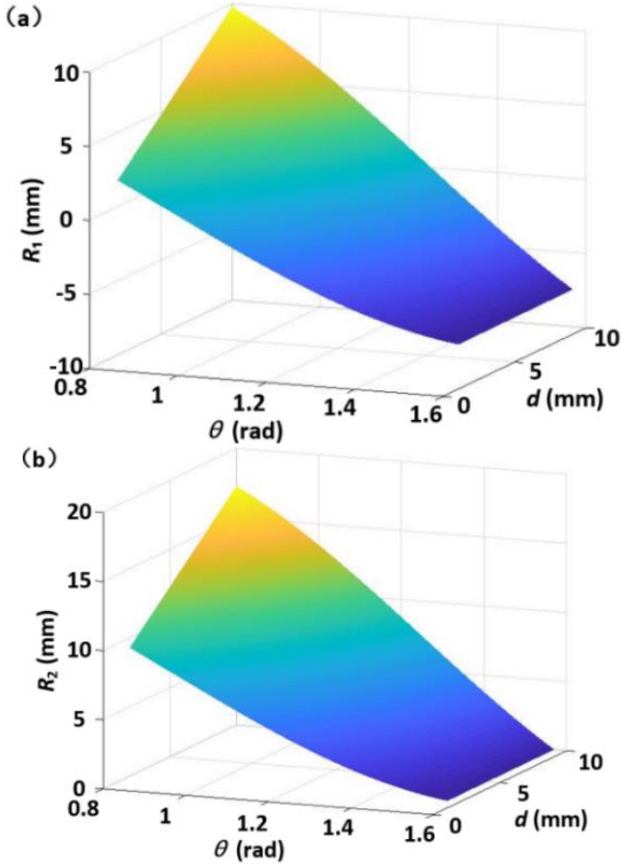

Fig. 5. (a) The relationship between θ, d and R1 when r=7.5 mm. (b) The relationship between θ, d and R2 when r=7.5 mm (color online)

As can be seen in Fig. 5, when θ is less than a certain range, R_2 is greater than 15 mm and the beam will be blocked during transmission. When θ is greater than or equal to 1.5708 rad, the shape of the device changes and there is no reference. When d is too small to match θ, R_1 is less than 2.996 mm and a portion of the light in the center cannot be emitted from the exit plane during the transmission. At a suitable θ, the range of d (shown in Eq. (4)) can be calculated by the relationship between the parameters.

$$d\geq\frac{r}{\tan\theta}-\frac{H+r}{\tan 2\theta},\ 1.0472\ \text{rad}\leq\theta<1.5708\ \text{rad} \tag{4}$$

Although the hollow beam can reduce the energy loss of the traditional antenna, the hollow beam with too large or too small a radius can also result in a certain amount of energy loss. Therefore, the scatter plot of the beam in Fig. 6 is used to analyze the loss of transmission efficiency.

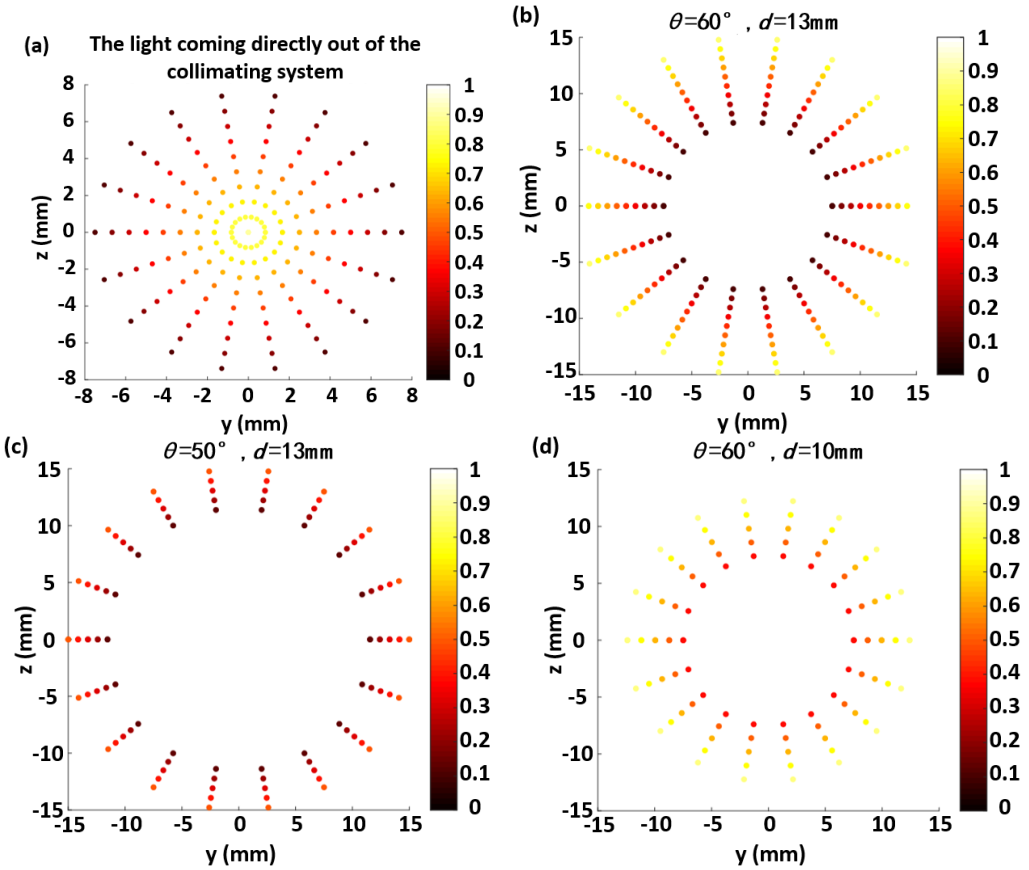

Fig. 6. (a) Scattering diagram of normalized energy of incident beam. (b) Scattering diagram at appropriate values. (c) Scattering diagram when θ is too small. (d) Scattering diagram when d is too small (color online)

As shown in Fig. 6 and Eq. (4), a reasonable arrangement of the values of θ and d allows all the beams to enter the lens. All considered, the scheme is set to 1.0472 rad for θ and 13 mm for d. In addition, the energy of the beam is reversed after passing through the D-R system. The farther the beam is from the main axis, the higher the light energy is. When the angle θ is less than 1.0472 rad, the light from the central part is reflected to the first reflecting surface on the other side of the device and cannot reach the second reflecting surface. When d does not satisfy the Eq. (4), the light from the edge part reaches the incident surface after the first reflecting surface and returns to the original way, resulting the light from that part not entering the lens.

4. Analysis of factors affecting transmission efficiency

After designing the D-R system, the transmission efficiency of the antenna with D-R system should be evaluated. Therefore, the known lens parameters of the Cassegrain antenna can more accurately model the path of the antenna, as shown in Table 1.

With the parameters in Table 1 and the parameters in the D-R system, three-dimensional light tracking diagram of the entire system is drawn, as shown in the Fig. 7.

Table 1. Parameter and formula of Cassegrain antenna

Curves of Surface	Radius of Rotation (mm)	Focal Length (mm)	Equation
Secondary mirror	15	240	$y^2 + z^2 = 480(x - 480)$
Primary mirror	75	1200	$y^2 + z^2 = 2400x$

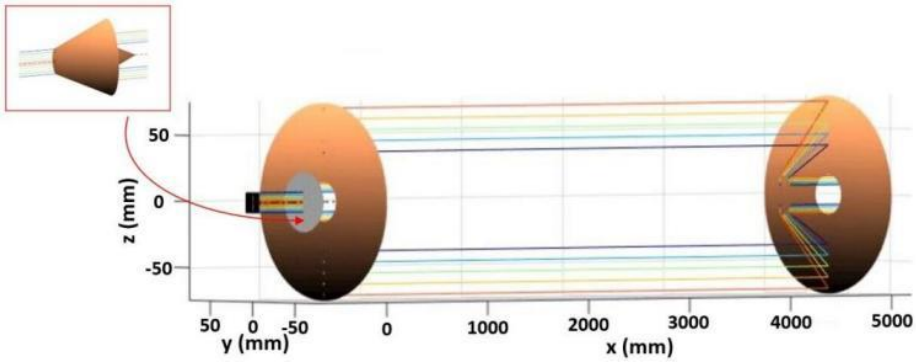

Fig. 7. Three-dimensional light tracing map of the entire system (color online)

It can be seen from Fig. 7 that the hollow beam formed by the D-R system can effectively reach the receiving system. Since the incident beam is a Gaussian beam, the formula for the energy distribution of the Gaussian beam (as shown in Eq. (5)) can be used to solve the transmission efficiency of the entire system.

$$|E(z)|^2 = \exp(-\frac{2r^2}{w^2(z)}) \tag{5}$$

where the waist radius ω_0 =10 mm. In addition to the solid beam, there are other practical factors that affect the transmission efficiency during the antenna transmission, such as transmission, chamfering, spindle offset, radius of incident beam, etc. The above factors will be analyzed and studied in the following using Eq. (5).

4.1. Dispersion

The D-R system consists of a common lens material and fiber optic reflectors. The beam is incident vertically from the incident plane and exits vertically from the exit plane by passing through two reflective surfaces.

As we know, the refractive index varies with the wavelength of the incident light. Since the beam enters the D-R system vertically, the different wavelengths of the incident beam affect the refractive index of the lens material, but do not alter the transmission path of the light within the lens. Because the fiber optic reflector enables complete reflection of light in the optical communication wavelength, the beam has no loss during the two reflections. In conclusion, the D-R system effectively avoids the influence of dispersion on transmission efficiency.

4.2. Reflectivity and transmittance

To improve the transmittance of the D-R system, a double-layered porous structure can be obtained by a broadband anti-reflection effect in the NIR region in a humid environment. Because of the high porosity of the top layer and the small porosity of the bottom layer, the reflectance of the film in the NIR region is less than 1% [13]. Therefore, the research group chose to coat the transmission surface of the D-R system with a double-layer porous film, where the beam enters and exits the D-R system. In this D-R system, the beam only passes through these two surfaces, so the efficiency of the transmitted part is shown in the Eq. (6).

$$\eta_c = (1-R_f)^N = (1-1.00\%)^2 = 98.01\% \tag{6}$$

where R_f is the reflectivity of the film, and N is the number of times the beam passes through the surface.

On the other hand, photonic crystal multilayer films can be used to improve the reflectivity of the D-R system. By choosing appropriate media (titanium dioxide and yttrium sulfate), we can obtain the normalized frequency range and corresponding wavelength range [9]. Since this wavelength range (1359-1673 nm) includes the optical communication wavelength of 1550 nm, TE polarized light and TM polarized light of light can achieve total reflection on each reflection surface during transmission.

4.3. Chamfering

When the center of the incident beam enters the D-R system through an acute angle, whose trajectory is difficult to determine. Therefore, chamfering is introduced to ascertain all ray trajectories [14]. As shown in Fig. 8, the top corner of the cone is replaced with a circular cap of radius r_c.

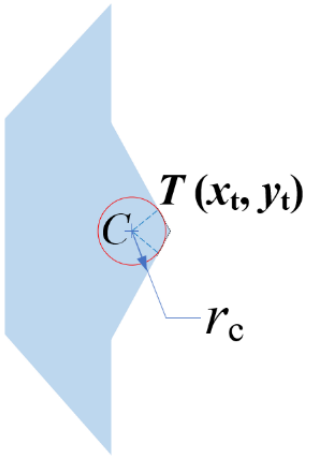

Fig. 8. D-R system with chamfer (color online)

The introduction of top chamfer will lead to a partial energy loss of the beam, which is investigated in the following part. The Eq. (7) is the chamfer formula about chamfering.

$$\begin{cases} L: y - y_t = k_t(x - x_t) \\ C: (x - x_c)^2 + (y - y_c)^2 = r_c^2 \end{cases} \tag{7}$$

where r_c is set as 0.5 mm, T (x_t, y_t) is the point where the chamfered circle is tangent to the lens, C (x_c, y_c) is the center of a chamfered circle. According to the properties of chamfering, the loss efficiency of the incident beam after chamfering is calculated as shown in the Eq. (8).

$$\eta_{lost} = \frac{\int_0^{2\pi}\int_0^{y_t} \exp(-\frac{2r^2}{w^2(z)})r\mathrm{d}r\mathrm{d}\theta}{\int_0^{2\pi}\int_0^{d} \exp(-\frac{2r^2}{w^2(z)})r\mathrm{d}r\mathrm{d}\theta} = 0.605\% \tag{8}$$

4.4. Radius of incident beam

After determining the parameters of the D-R system, most solid beams of different radii can be passed. When the radius of incident beam is less than the bottom radius H of the system, the energy distribution received by the lens is shown in the Fig. 9.

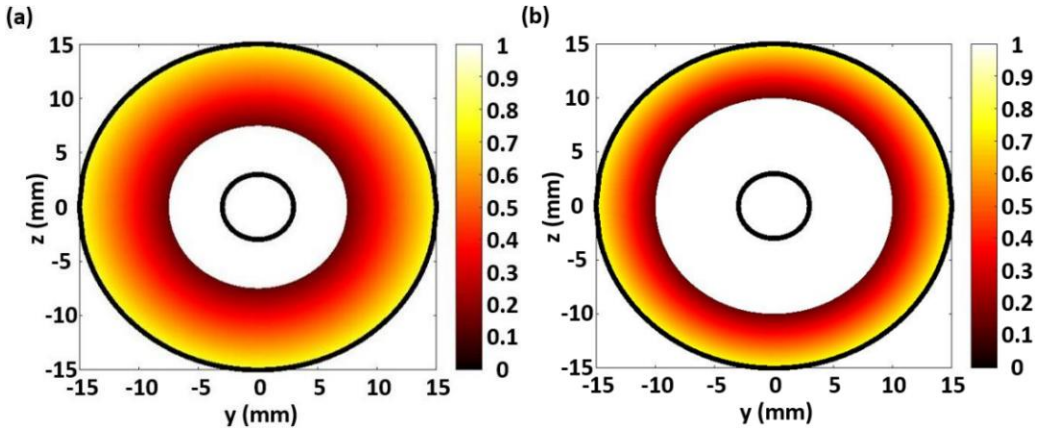

Fig. 9. Effects of different parameter values on transmission efficiency in D-R system. The radius of the two black circles are 2.996 mm and 15 mm. (a) Energy distribution of the outgoing beam when r=7.5 mm. (b) Energy distribution of the outgoing beam when r<7.5 mm (color online)

The Fig. 9 illustrates that when $r \leq 7.5$ mm, all the energy of the incident beam reaches the transmit antenna. However, when the radius of the incident beam exceeds a certain range, the peripheral light is reflected from the second reflecting surface and cannot enter the D-R system. The energy of light entering the D-R system is analyzed and the transmission efficiency of light is calculated as Eq. (9).

$$\eta_p = \frac{\int_0^{2\pi}\int_0^{H} |E|^2 r\mathrm{d}r\mathrm{d}\theta}{\int_0^{2\pi}\int_0^{r} |E|^2 r\mathrm{d}r\mathrm{d}\theta} \tag{9}$$

where the meanings of H and r are shown in Fig. 3. To observe the variation of the transmission efficiency more visually, Fig. 10 simulates the relationship between the transmission efficiency and the radius of incident beam.

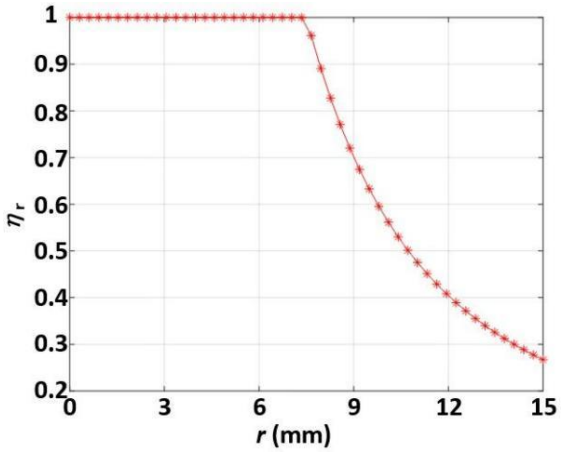

Fig. 10. Diagram of transmission efficiency versus incident beam radius (color online)

Fig. 10 reveals that when the radius of incident beam r is between 0 and 7.5 mm, all exit rays can reach the main reflector through the secondary reflector of the D-R system. When r > 7.5 mm, the transmission efficiency gradually decreases with the increase of r.

4.5. Spindle deviation

It is well known that the transmitting and the receiving antennas are often far apart, which means that the main axes of both do not coincide completely in most cases. The slight deviation of the main axes has some effect on the transmission of the antenna and prevents the receiving system from fully receiving all the energy [15].

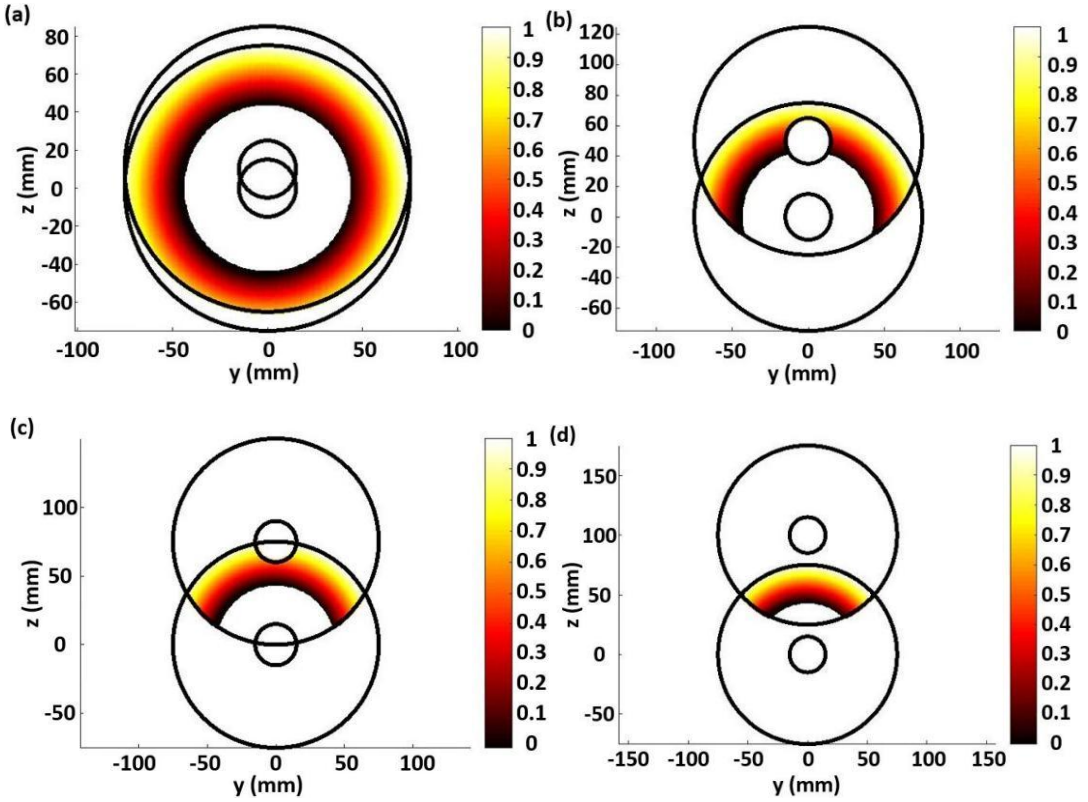

Fig. 11. Energy acceptance diagram of a receiving system with different optical axis deviation distances (color online)

The simulation Fig. 11 reveals that the receiving system receives less light when the spindle deviation distance between the transmitting and receiving system is larger. The relationship between the transmission efficiency and the spindle deviation distance D is obtained by calculation and simulation (see Fig. 12).

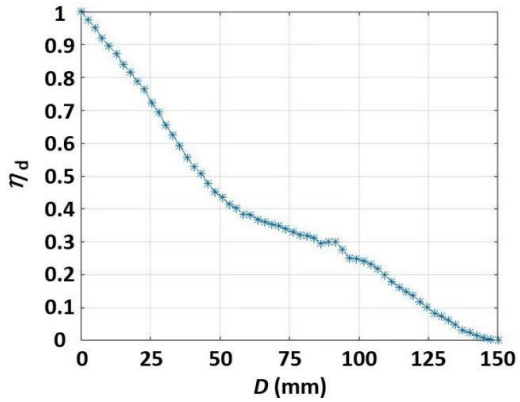

Fig. 12. Diagram of the relationship between transmission efficiency and spindle deviation (color online)

Theoretically, the transmission efficiency should be smaller when the spindle offset is larger. Furthermore, as can be seen in Fig. 12, there are some anomalous trends (smaller increases in some regions) throughout the descent due to the uneven distribution of light energy.

4.6. The transmission efficiency of the whole system

Combined with the above equations and figures, all the energy reaches the receiving system after the D-R system converts the solid beam into the hollow beam. In other words, the D-R system can achieve 100% transmission efficiency under ideal conditions. Taking the upper chamfering, refraction and transmission factors into account, and ensuring that the incident beam radius is within a reasonable range, the transmission efficiency of the scheme remains high, which is shown in Eq. (10).

$$\eta_{novel} = (1-\eta_{lost})\eta_c = 97.42\% \tag{10}$$

Considering the offset distance of the spindle of the transmitting and receiving systems, a practical transmission efficiency diagram can be obtained as follows:

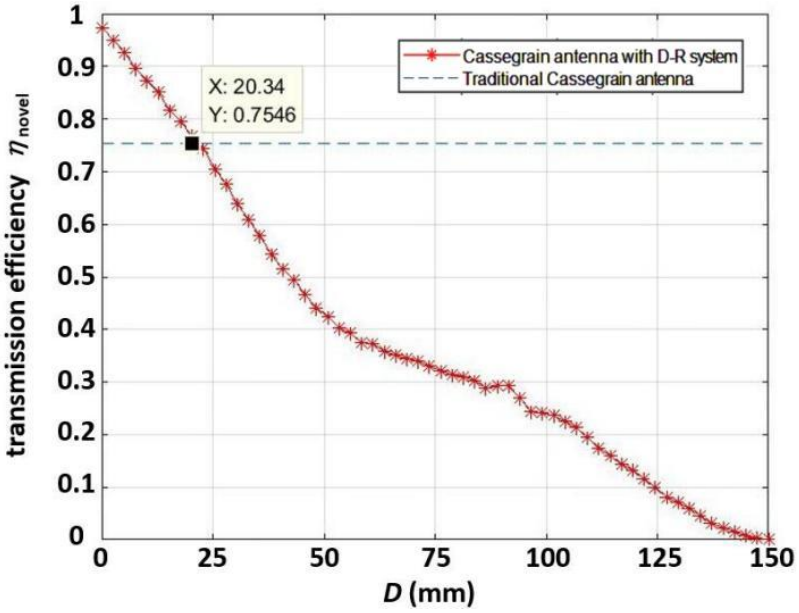

Fig. 13. Diagram of practical transmission efficiency versus spindle deviation (color online)

From the comparison in the Fig. 13, when the spindle offset value D is less than 20.34 mm, the transmission efficiency is higher than the transmission efficiency of 75.46% of the traditional Cassegrain antenna [10]. Therefore, this scheme can improve the transmission efficiency of Cassegrain antenna well.

5. Conclusion

In this paper, we design the D-R system, a scheme to improve the transmission efficiency of Cassegrain antennas by converting solid beams into hollow beams. Based on the three-dimensional vector reflection theorem, the parameters H=7.5 mm, θ=1.0472 rad and d=13 mm are reasonably set. According to our simulation results, under ideal conditions, the D-R system can improve the transmission efficiency of traditional Cassegrain antenna up to 100%. After taking several factors such as dispersion, chamfering, radius of incident beam, spindle deviation, reflectivity and transmittance into consideration, the D-R system can still improve the transmission efficiency of traditional Cassegrain antenna up to 97.42%. In addition, the transmission efficiency of the whole system is higher than the transmission efficiency of the traditional Cassegrain antenna under an axes offset between 0 and 20.34 mm. The proposed antenna with D-R system possesses a relatively simple structure and adequate fault tolerance.

References

[1] D. Q. Su, H. Bai, X. Q. Cui, Research in Astronomy and Astrophysics **20**, 1 (2020).
[2] H. A. Junior, F. J. S. Moreira, 2021 SBMO/IEEE MTT-S International Microwave and Optoelectronics Conference (IMOC) 1 (2021).
[3] A. Sharifi, IETE Journal of Research **69**, 410 (2023).
[4] S. A. H. Mohsan, N. Q. H. Othman, M. Uddin, Z. Elahi, 2021 Photonics and Electromagnetics Research Symposium (PIERS), 1359 (2021).
[5] L. Zhang, Lu Chen, H. J. Yang, P. Jiang, S. Q. Mao, W. N. Caiyang, Appl. Opt. **54**, 7148 (2015).
[6] B. Cao, P. Jiang, J. Y. Wang, S. Q. Mao, W. N. Caiyang, Y. Qin, H. J. Yang, Appl. Opt. **58**, 1356 (2019).
[7] R. X. Liu, H. J. Yang, P. Jiang, Y. Qin, W. N. Caiyang, B. Cao, M. F. Zhou, S. Q. Mao, Appl. Opt. **59**, 3736 (2020).
[8] Y. Qin, H. J. Yang, P. Jiang, W. N. Caiyang, M. F. Zhou, S. Q. Mao, B. Cao, Opt. Express **28**, 14436 (2020).
[9] M. F. Zhou, H. J. Yang, P. Jiang, Y. Qin, W. N. Caiyang, S. Q. Mao, B. Cao, Appl. Opt. **58**, 3410 (2019).
[10] X. R, Zhang, H. J. Yang, P. Jiang, M. F. Zhou, W. N. Caiyang, Y. Qin, B. Cao, Appl. Opt. **60**, 6829 (2021).
[11] J. Zhao, H. Yang, R. Chen, Y. Wang, P. Jiang, Optik **126**, 2059 (2015).
[12] B. Cao, P. Jiang, H. J. Yang, Y. Qin, M. F. Zhou, Opt. Commun. **493**, 127029 (2021).
[13] M. F. Zhou, H. J. Yang, P. Jiang, W. N. Caiyang, Y. Qin, B. Cao, Applied Optics and Photonics China (AOPC 2020) **11568**, 1 (2020).
[14] X. Chen, H. J. Yang, P. Jiang, J. J. Wang, W. N. Caiyang, J. Optoelectron. Adv. M. **19**(3-4), 132 (2017).
[15] L. Z. Hu, P. Jiang, H. J. Yang, Y. Qin, W. N. Caiyang, Y. F. Zheng, J. X. Deng, J. Y. He, J. Yang, Optics Communications **526**, 128906 (2023).

*Corresponding author: yanghj@uestc.edu.cn